

Cite this: *J. Mater. Chem. C*, 2014, 2, 5533

Thiol–ene photo-curable hybrid silicone resin for LED encapsulation: enhancement of light extraction efficiency by facile self-keeping hemisphere coating†

Yanchang Gan, Xuesong Jiang* and Jie Yin

Encapsulation with polymer materials can not only protect LED chips, but also enhance light extraction efficiency (LEE), and thus it has become necessary for the fabrication of LED devices. We developed a new concept of LED encapsulation with photo-curable hybrid silicone resin, which allows facile encapsulation at room temperature. The photo-curable silicone liquid resin based on thiol–ene photopolymerization is comprised of styrene-modified mercaptopropyl-polysilsesquioxane (St-POSS-SH) with a ladder-like polysilsesquioxane containing acrylic and phenethyl sulfide groups (LPSQ). Even under open air condition, the resulting liquid silicone resin can be photo-cured in 2 minutes at room temperature, and can keep a hemisphere shape during encapsulation without a mold. The optical, mechanical and thermal properties of the resulting cured silicone resin were evaluated in detail. The silicone resin is transparent and possesses a high refractive index of 1.545 (@450 nm). The encapsulation of blue GaN LED with this self-keeping hemisphere-shaped photo-cured silicone resin achieved a LEE enhancement of 25.6%, compared to flat encapsulation induced by heat. Contrary to thermal encapsulation, the encapsulation of an LED chip with the photo-curable silicone resin does not involve the processes of mold and demold, which simplifies the LED encapsulation procedure, and obviously decreases the operation cost. We believe that this novel photo-curable silicone resin based on thiol–ene photopolymerization will greatly improve the encapsulation of LED chips.

Received 21st February 2014
Accepted 13th May 2014

DOI: 10.1039/c4tc00350k

www.rsc.org/MaterialsC

1. Introduction

GaN-based light-emitting diodes (LEDs) are an attractive light source for illumination or display signs because of their long lifetime and high efficiency compared to those of conventional light sources.^{1,2} Although high LED efficiency can be obtained by improvements of internal quantum efficiency, the occurrence of trapped light inside a high-refractive-index semiconductor remains one of the fundamental challenges. The total internal reflection (TIR) severely reduces the light-extraction efficiency (LEE) of LEDs.^{3–7} As for the commercial flip GaN/InGaN-based LEDs usually built on the sapphire substrate, the bare uncoated sapphire surface exhibits a high refractive index of 1.76 compared to air (1.0), which means that considerable light is reflected back into sapphire at the sapphire/air interface, according to the Snell's law. Taking the planar uncoated bottom-emitting LED chip as an example, the light emitted only

in the cone shape, referred as the light-escape cone, can escape outside into the air (Fig. 1a). The light cone⁴ is defined as the boundary surrounded by the total refraction, and the maximum angle of incidence is referred to as the critical angle (θ_c).

To overcome this challenge of TIR, LED chips are usually encapsulated in transparent polymer material, which increases θ_c and protects the chips (Fig. 1b). The addition of an encapsulant to LED chips creates two interfaces: sapphire substrate/encapsulant and encapsulant/air. The reflection loss at the sapphire substrate/encapsulant interface is decreased by the high refractive index of polymer encapsulant.⁶ Fresnel reflection loss at the encapsulant/air interface is reduced by the hemisphere shape of the encapsulant (Fig. 1c).⁶ In industry, for practical LED encapsulation, the commercial thermal-cured silicone resin is shaped into the hemisphere using a mold to reduce Fresnel reflection loss at the encapsulant/air interface. Due to the low viscosity and good mobility of the thermal-curing resin at the high temperature (usually around 150 °C for one hour), the encapsulation shape of silicone resin is often flat and cannot take the shape of a hemisphere without the help of the mold (Fig. 1d). Therefore, two steps of mold and demold are necessary in the present thermal-encapsulation of LED chips in industry. However, the multiple steps of the encapsulation

School of Chemistry & Chemical Engineering, State Key Laboratory for Metal Matrix Composite Materials, Shanghai Jiao Tong University, Shanghai 200240, People's Republic of China. E-mail: ponygle@sjtu.edu.cn; Fax: +86-21-54747445; Tel: +86-21-54743268

† Electronic supplementary information (ESI) available. See DOI: 10.1039/c4tc00350k

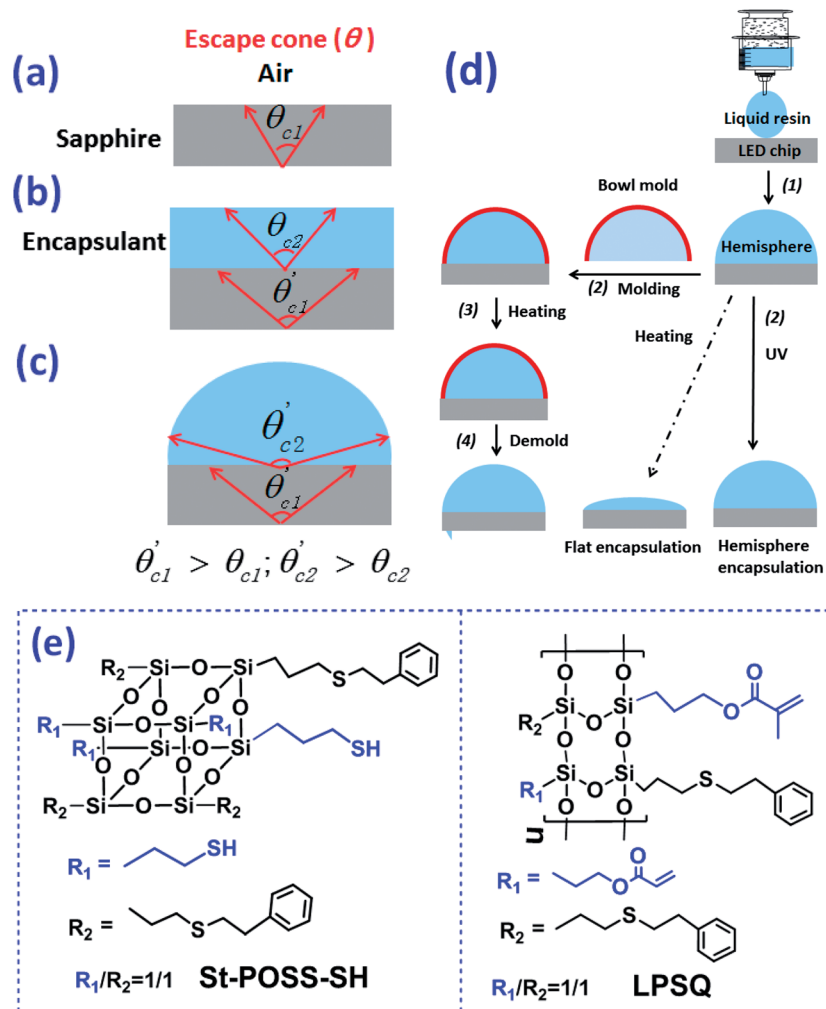


Fig. 1 Schematic diagrams of LED chip encapsulation to enhance LEE (a–c): the light-escape cone of the bare LED chip from the sapphire to air increases after encapsulation. The light loss at the encapsulant/air interface is reduced by a hemisphere-shaped encapsulant. (d) Comparison of the thermal- and photo-encapsulation of LED chips: the commercial thermal-encapsulation requires four steps, including of mold and demold, to form the hemisphere-shaped encapsulant, compared to only two steps for encapsulation with photo-curable resin at room temperature. (e) The chemical structure of the two components of the photo-curable silicone resin.

process with thermal-cured silicone resin, including mold and demold, reduce the efficiency of encapsulation and increase the operation cost.

We present herein a new concept of facile LED encapsulation with photo-cured silicone resin, instead of thermal-cured resin (Fig. 1d). The photo-polymerization is much faster and can be carried out at lower temperatures, compared to thermal polymerization.⁸ The viscous silicone liquid resin can self-form a hemispherical drop on the limited sapphire substrate due to surface tension at low temperatures.⁹ Upon irradiation with UV light at room temperature (RM), the liquid silicone resin is cross-linked to the polymer network, which can keep the initial hemisphere shape without the help of a mold. Thus, we call the photo-cured encapsulation as the self-keeping hemisphere coating. The encapsulation procedure with photo-cured resin does not involve mold and demold steps like thermal encapsulation, which simplifies the encapsulation procedure of LED chips and decreases operation cost (Fig. 1d). Besides this

significant advantage, LEDs RM-encapsulated with photo-cured resin avoid the damage caused by high temperature during thermal encapsulation. The chemical structures of the two components of photo-cured silicone resin for LED chip encapsulation are shown in Fig. 1e. After deposition on the naked LED chip, the hemispherical liquid silicone resin can be photo-cured in 2 minutes at room temperature. It is shown that GaN LED with this hemispherical encapsulant can achieve a LEE enhancement of 25.6%, compared to the LED chip with flat coating due to a reduced Fresnel reflection loss at the encapsulant/air interface.

2. Results and discussion

2.1 Design and cross-linking kinetics of thiol-ene photo-curable silicone resin

A number of physical and chemical features were considered in the design of the chemistry and materials to encapsulate LED

chips. Silicone hybrid resin is one of the considered materials for the encapsulation of LED chips due to its high optical transparency, chemical and physiological stability, fracture resistance, and minimal moisture absorption.^{10–12} Therefore, thermal-curable silicone is widely used as LED encapsulant for high performance. The resin is formed by two components cured at high temperature in the presence of chloroplatinic acid (H₂PtCl₆) as catalyst.¹³ As shown in Fig. 1e, our photo-cured resin is also based on silicone combining styrene-modified mercaptopropyl-polsilsesquioxane (St-POSS-SH) with a polysilsesquioxane ladder of acrylic and phenethyl sulfide groups (LPSQ). Details on the synthesis and structural characterization of St-POSS-SH and LPSQ can be found in Supporting Information (Fig. S1–S6†). POSS is considered an organic–inorganic hybrid material at the molecular level, and the incorporation of POSS imparts excellent mechanical and thermal properties to the resulting material.^{14–17} The ladder-like polysilsesquioxanes can be used as matrix and might surpass the performance of linear polysilsesquioxanes regarding some of the properties, such as thermal stability.^{18,19} St-POSS-SH and LPSQ are silicone cross-linkers and silicone monomers, respectively. The introduction of phenethyl sulfide groups not only increases compatibility between St-POSS-SH and LPSQ, but also increases the refractive index of the hybrid silicone material.²⁰ Upon UV-light irradiation at room temperature, our silicone resin is photo-cured by thiol–ene polymerization, instead of the conventional radical photopolymerization. Besides the significant advantage of less oxygen inhibition over the conventional radical polymerization, thiol–ene polymerization leads to fast curing, low shrinkage and stress, and homogeneous mechanical properties.^{20–26} Furthermore, the induction of sulfur atoms can increase the refractive index of the resulting encapsulant,^{20,27} which is favorable for light extraction.

The optimal formulation of the LED chip encapsulant was found by preparing a series of liquid mixtures with different ratios of St-POSS-SH and LPSQ, and by comparing their performance (Table 1). The as-prepared St-POSS-SH/LPSQ mixtures with different ratios are transparent liquids, meaning an excellent compatibility between St-POSS-SH and LPSQ. This compatibility is an important factor for the performance of the resulting cross-linked materials, especially for optical transparency. The same phenyl side groups and hybrid polysilsesquioxane backbone in both St-POSS-SH and LPSQ might be responsible for the good compatibility.

The curing-reaction kinetic of liquid resin is an important parameter of the LED chip encapsulation procedure. We first used real-time FT-IR to study the photopolymerization kinetic of St-POSS-SH/LPSQ resin containing trace amounts of photo-initiator. We monitored change in the peak at 1630 cm⁻¹ corresponding to ene (C=C), and peak at 2555 cm⁻¹ corresponding to thiol (–SH) (Fig. 2a and b). Upon UV-light irradiation at 365 nm with an intensity of 40 mW cm⁻², all mixtures of liquid resin were photo-cured at room temperature and open air. The photo-curing reaction of all formulations was fast, and the balanced conversion of the C=C was achieved within the first 100 seconds (Fig. 2a). For St-POSS-SH/LPSQ with thiol–ene = 1/1, the C=C conversion was higher than 92% after 60 s irradiation. The final conversion of –SH for all formulation was as high as 90%, while the final conversion of C=C decreased from 92% to 40% with decreasing ratios of thiol–ene from 1/1 to 0/1. For photo-curing of pure LPSQ (St-POSS-SH/LPSQ-0/1), the oxygen quenching of the active radicals might lead to the low conversion of C=C due to the absence of thiol groups. These data show the positive effect of thiol groups on photo-polymerization, and are consistent with the previous studies on thiol–ene photo-curing systems.

The photo-curing kinetic of St-POSS-SH/LPSQ was also investigated by photo-differential scanning calorimetry (photo-DSC). As shown in Fig. 2c, the maximum heat flow (H_{f,max}) increased from 4.7 to 10.7 mW mg⁻¹, while the time corresponding to H_{f,max} (T_{max}) decreased from 13.4 s to 12.7 s, with increasing ratios of thiol–ene from 0/1 to 1/1. As main factors in the rate of photo-polymerization, both higher H_{f,max} and shorter T_{max} yield faster photopolymerization. Thus, these photo-DSC data show that thiol–ene photopolymerization of St-POSS-SH/LPSQ-1/1 is faster than that of pure LPSQ. According to the amount of heat liberated, the conversion of C=C double bond increased from 41% to 93% with the addition of St-POSS-SH, which is in good agreement with the FT-IR results. The investigation of photo-curing kinetics indicated that our St-POSS-SH/LPSQ resin can be cured rapidly by UV-light exposure even in open air, which makes LED chip encapsulation very feasible and convenient. To better understand oxygen inhibition in the air, we compared the properties of our silicone resin photopolymerized in air or nitrogen gas (Fig. 3). The photo-curing behavior of St-POSS-SH/LPSQ-1/1 under these two conditions was almost the same, and C=C conversion >90% can be achieved after UV-exposure of 60 s. These results confirm

Table 1 Formulation and physical properties of the photo-cured hybrid silicone resin. All samples were UV irradiated at 365 nm and an intensity of 40 mW cm⁻² for 300 s at room temperature

St-POSS-SH/LPSQ (mol mol ⁻¹)	Shrinkage (%)	Young's modulus (GPa)	Hardness (MPa)	T _d ^a (°C)	T _g (°C)	RI (450 nm)	T% ^b (450 nm)
1/1	2.1	0.16	27	325	–22	1.549	93
1/1.5	3.1	0.21	29	330	–27	1.535	93
1/2	3.5	0.30	35	336	–32	1.532	93
1/4	4.2	0.50	50	338	–36	1.529	93
0/1	5.1	0.59	65	340	–39	1.525	94

^a Temperature at the 5% loss weight of the resin network. ^b The thickness of the film was around 800 μm.

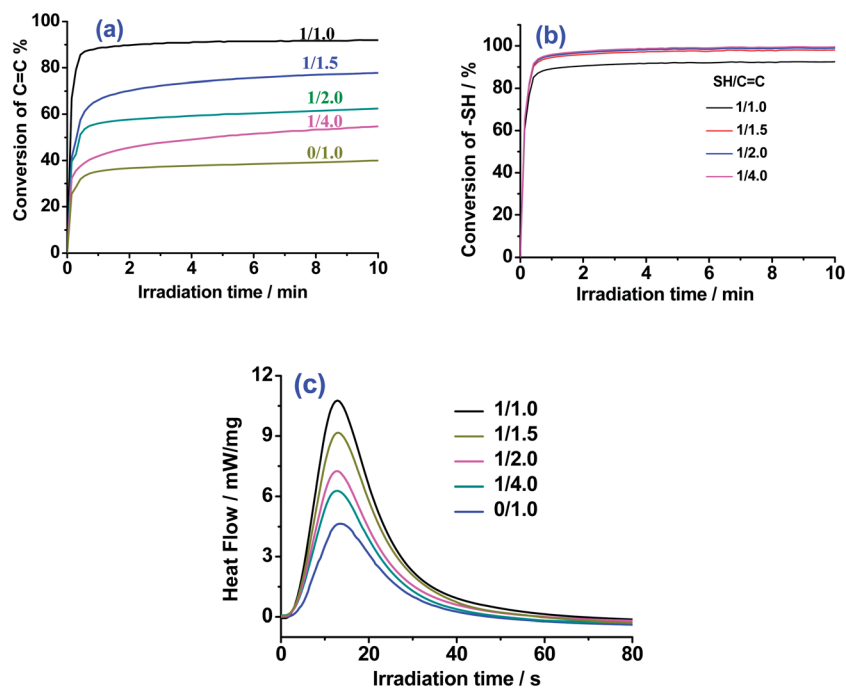


Fig. 2 Conversion of (a) C=C and (b) -SH during the polymerization of St-POSS-SH/LPSQ resins determined by real-time FT-IR. (c) Photo-DSC exotherms for the photopolymerization of St-POSS-SH/LPSQ resins. All samples were UV irradiated at 365 nm, with an intensity of 40 mW cm^{-2} , at room temperature, and open air. Photoinitiator content was fixed at 5 wt% LPSQ.

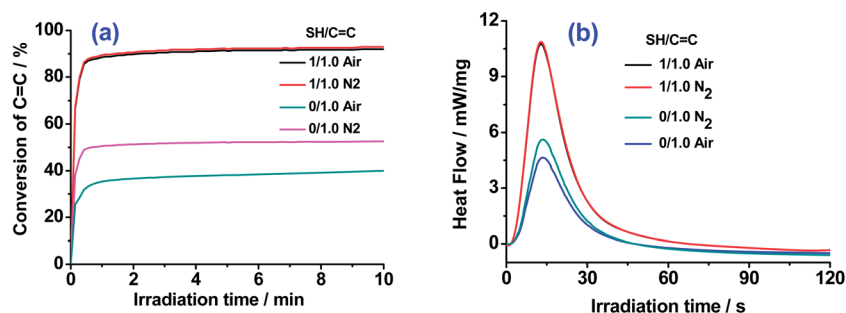


Fig. 3 (a) Real time FT-IR conversion of -C=C- during the polymerization St-POSS-SH/LPSQ (1/1.0) and pure LPSQ resin under air or N_2 environment. (b) Photo-DSC photopolymerization exotherms of St-POSS-SH/LPSQ (1/1.0) and pure LPSQ resins under air or N_2 environment. In both experiments, the photoinitiator content was fixed at 5 wt% LPSQ resin and light intensity at 40 mW cm^{-2} .

that oxygen inhibition is negligible during photo-curing of St-POSS-SH/LPSQ-1/1. This should be ascribed to the inherent advantage of thiol-ene photopolymerization: thiol groups can weaken the quenching effect of oxygen on the active radicals generated in the system.²⁸ In contrast, the final conversion of C=C and maximum heat flow during the photopolymerization of pure LPSQ increased significantly under nitrogen gas, suggesting oxygen-inhibition during conventional radical polymerization. Another major feature of our St-POSS-SH/LPSQ resin is its reduced volumetric shrinkage. After photo-curing, the volume shrinkage of the film decreased with increasing content in St-POSS-SH. The volume shrinkage of St-POSS-SH/LPSQ-1/1 resin was around 2.1%, which is less than with pure LPSQ (5.1%).

2.2 Optical, thermal and mechanical properties

We then studied the performance of the photo-cured St-POSS-SH/LPSQ films as LED chip encapsulant including the optical, mechanical, and thermal properties. As shown in Fig. 4a, all St-POSS-SH/LPSQ films were homogeneous, colorless and transparent, suggesting no phase separation on a scale greater than the wavelength of visible light. This might be ascribed to the good compatibility between St-POSS-SH and LPSQ. The light transmittance of the 800 μm -thick films is as high as 93% over the entire range of visible light (380–800 nm). The refractive index (RI) for all films is higher than 1.515 for the entire visible range, which might be due to the introduction of phenyl rings and sulfur atoms. The RI of the resulting film increased with the increasing content of St-POSS-SH, and the St-POSS-SH/LPSQ-1/1

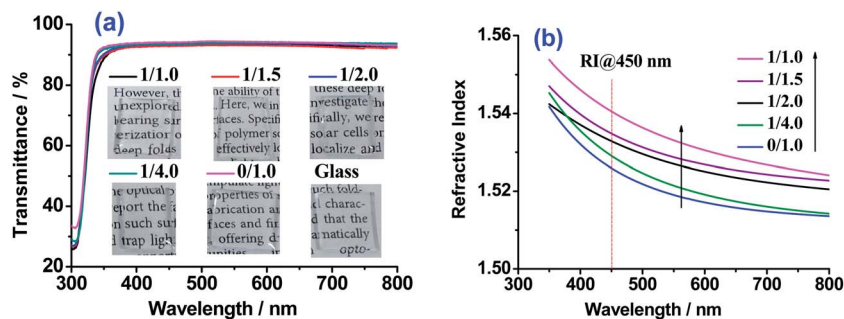


Fig. 4 Transmittance curves (a) and refractive index curves (b) of the UV-cured St-POSS-SH/LPSQ film. The thickness of film is around 800 μm .

film exhibited the highest RI of 1.545 at 450 nm. The enhancement of RI by St-POSS-SH might be ascribed to the introduction of sulfur atoms due to the well-known heavy atom effect.²⁷ As the RI of the LED chip substrate is usually much higher than that of polymer encapsulant (for example, RI of sapphire is 1.760 (ref. 29)), the higher RI of encapsulant can decrease the reflection loss at the substrate/encapsulant interface.

Thermogravimetric analysis (TGA) and DSC (Table 1 and Fig. 5) were carried out to obtain information regarding the thermal stability of the photo-cured St-POSS-SH/LPSQ film. All these films possessed an initial decomposition temperature (T_d) higher than 320 $^{\circ}\text{C}$. The glass transition temperature (T_g) increased with the increasing St-POSS-SH content. The enhancement of T_g by the introduction of St-POSS-SH can be explained by the POSS characteristic of inorganic nanoparticles. The Young's modulus and hardness of the cured film, determined by the nanoindentation test, decreased with the increasing St-POSS-SH content. Young's modulus and hardness of the St-POSS-SH/LPSQ-1/1 film without any reinforcing agent were still 160 MPa and 27 MPa, respectively, which are much higher than that of PDMS (0.2–1.8 MPa).^{30,31} Based on these results, including the photo-curing kinetics, optical, thermal, and mechanical performance, St-POSS-SH/LPSQ-1/1 resin was chosen as LED chip encapsulant in the following device studies.

2.3 Encapsulation of LED chip

To demonstrate the feasibility of our photo-cured silicone resin for LED chip encapsulation, flip blue GaN LED chips

($\lambda = 450 \text{ nm}$, $3 \times 3 \text{ mm}$) with the sapphire substrate were drop coated with a fixed volume of St-POSS-SH/LPSQ-1/1 liquid resin (Fig. 1d and 6a). The surface tension of the viscous liquid silicone resulted in a hemispherical liquid drop on the small LED chips surface. Upon direct irradiation with 365 nm UV light for 5 minutes at room temperature, the liquid drop became completely solid and maintained a hemispherical shape on the sapphire substrate (Fig. 6b, inset). The hemispherical package was difficult to detach from the LED chip, indicating good adhesion between the silicone resin and the LED chip. This might be ascribed to the presence of sulfur atoms, which can enhance the adhesion of silicon resin to the inorganic substrate. When the coated LED chip was thermal-cured using the commercial conditions (150 $^{\circ}\text{C}$ for 60 min), the coating on the sapphire substrate became almost flat because the liquid drop flowed out of the small surface at the high temperature. A similar thermal reaction was observed with the commercial thermal-curable silicone resin (e.g. Dowcorning 6550). For direct comparison and analysis, we defined θ_e as the encapsulated angle, which is the contact angle of the liquid resin drop on the sapphire substrate (Fig. 6b, inset). We compared the electroluminescence spectra generated by unencapsulated LED chips (reference), or after hemispherical or flat encapsulation, under DC current injection of 350 mA and light output power. As shown in Fig. 6c and d, the LEE and light output power of the LED chip increased after encapsulation with silicone resin. The LED chips with flat and hemispherical encapsulation exhibited 4.3% (5.6% for Dowcorning 6550 flat encapsulation, showing in Fig. S7†) and 26.3% higher LEE than that of the naked LED chip. The significant LEE enhancement by the hemispherical

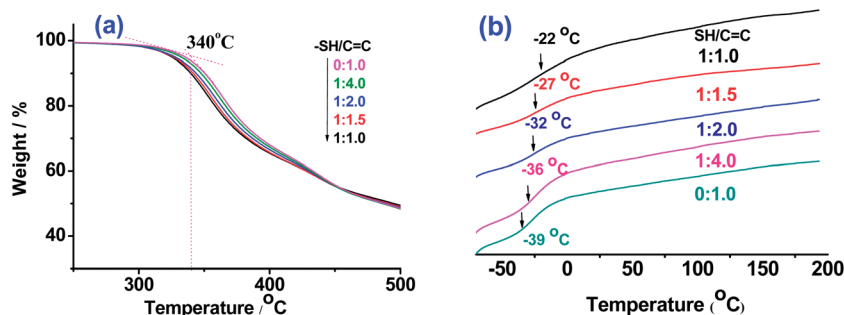


Fig. 5 TGA (a) and DSC (b) curves of cured St-POSS-SH/LPSQ film with molar ratios of thiol-ene at 1/1.0, 1/1.5, 1/2.0, 1/4.0 and 0/1.0.

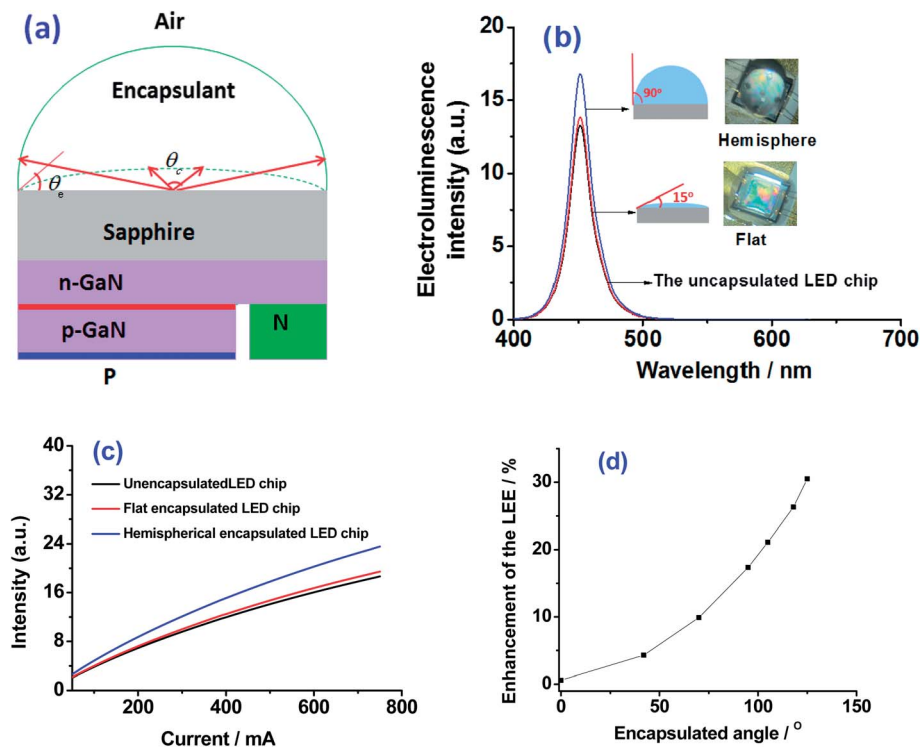


Fig. 6 (a): The flip GaN LED chip and its encapsulant with different encapsulation angles (θ_e); The electroluminescence spectra (b) and light output power versus forward drive current (c) of the flat and hemispherical encapsulated LED chips, as well as unencapsulated LED chip. The LED chip used for evaluation is the blue GaN LED chip ($\lambda = 450$ nm, 3×3 mm); (d) light extraction efficiency enhancement as a function of the encapsulated angle.

encapsulant can be explained by the lower Fresnel reflection loss at the curved encapsulant/air interface.

The impact of encapsulant shape on the light output power of LED chips was evaluated. The encapsulation angle was controlled by the amount of liquid resin dropped on the small sapphire surface. As shown in Fig. 6d, the LEE of the encapsulated LED chips increased with the increasing encapsulation angle. The enhancement of LEE by the encapsulation angle can be explained by the analysis of the model shown in Fig. 6a. The escape light cone at encapsulant/air interface is enhanced by the increasing encapsulation angle, resulting in lower Fresnel reflection loss. When the encapsulation angle is 90° , for example, all the light in the center area is perpendicular to the encapsulant/air interface, and can escape to the outside. If the encapsulant shape is hyper-hemispherical (θ_e), more light from the other area is emitted outside and the LEE of the encapsulated LED chip is enhanced by 30.7%.

To further understand the advantages of our photo-curable resin, we also encapsulated the blue LED chip by hemisphere-shaped thermal-encapsulation using commercial thermal-curable silicone resin (Dowcorning 6550) and a polycarbonate bowl as encapsulant and shape mold, respectively. As shown in Fig. S7,† the LEE enhancement of the hemispherical encapsulated LED chip with polycarbonate mold is around 25%, which is close to our self-keeping hemispherical encapsulation by photo-curable silicone resins.

3. Conclusion

We present a proof-of-concept that the new photo-curable silicone resin based on thiol-ene photopolymerization can realize facile encapsulation of LED chips at room temperature. The liquid silicone resin can be photo-cured in 2 minutes under open air at room temperature, and the resulting cured silicone possesses good optical, thermal and mechanical properties. The fast photo-curing at room temperature allows the liquid silicone resin to keep a hemispherical shape during encapsulation, without a mold. The encapsulation of blue GaN LED with the self-keeping hemisphere-shaped photo-cured silicone achieved a LEE enhancement of 25.6%, compared to thermal flat encapsulation. Contrary to thermal encapsulation, the encapsulation of LED chip with photo-curable silicone does not involve mold and demold processes, which simplifies the LED encapsulation procedure and considerably decreases the operation cost. This novel photo-curable silicone is very promising for the facile encapsulation of LED chips.

4. Experimental section

4.1 Measurement and characterization

^1H NMR and ^{29}Si NMR spectra were recorded on a Varian Mercury Plus-400 NMR spectrometer (400 MHz) with CDCl_3 as the deuterated solvent. FTIR spectra were recorded on a Perkin-Elmer Paragon 1000 FTIR spectrometer. Conversions were

calculated from the ratio of peak area measured after and prior to polymerization. Photopolymerization kinetics were measured by photo-DSC measurements (DSC 6200 Seiko Instrument) with a high-pressure mercury lamp as light source. TGA was performed in nitrogen with a Perkin-Elmer TGA 2050 instrument at a heating rate of 10 °C min⁻¹. Before each measurement, the samples were maintained at 100 °C under vacuum for 12 h to remove any solvent. The viscosity of the hybrid resins was determined at 25 °C using a NDJ-79 rotational viscometer. Measurements were acquired on 10–15 mL samples at a rotation speed of 5–75 rpm. The Young's modulus of the cured film was measured at room temperature with a commercial nanoindentation system (Hysitron TI-900 TriboIndenter, USA). According to ISO 3521, a pycnometer was used to measure the density (ρ) of uncured and cured resist specimens. The volumetric shrinkage was calculated using the formula: $\Delta V\% = \left(1 - \frac{\rho_{\text{uncured}}}{\rho_{\text{cured}}}\right) \times 100\%$.

4.2 Encapsulation and measurement of LED chip

An injection syringe was filled with St-POSS-SH/LPSQ-1/1 resins containing 5 wt% I907, and a fixed volume was dropped and adhered to the LED chips' small surface. Then, the LED chips covered with St-POSS-SH/LPSQ-1/1 resins were exposed to UV-irradiation (365 nm; 5 minutes) to obtain the self-keeping half-spherical encapsulation. The encapsulated angle was modified by changing the volume of the resin drop. The measurements of electroluminescence spectra and light output power were carried out in an integrating sphere system (HAAS-2000) assembled with a fiber spectrometer.

Details on the synthesis and characterization of St-POSS-SH and LPSQ can be found in ESI.†

Acknowledgements

We thank Hitachi-Chemical for financial support and Mr Kaji from Hitachi-Chemical for helpful discussions. We also thank the National Nature Science Foundation of China (21174085, 21274088, 51373098) for the financial support. X. S. Jiang is supported by the NCET-12-3050 Project.

References

- 1 F. A. Ponce and D. P. Bour, *Nature*, 1997, **386**, 351.
- 2 N. Holonyak, *Am. J. Phys.*, 2000, **68**, 864.
- 3 I. Schnitzer, E. Yablonovitch, C. Caneu and T. J. Gmitter, *Appl. Phys. Lett.*, 1993, **62**, 131.
- 4 I. Schnitzer, E. Yablonovitch, C. Caneu, T. J. Gmitter and A. Schere, *Appl. Phys. Lett.*, 1993, **63**, 2174.
- 5 T. Fujii, Y. Gao, R. Sharma, E. L. Hu, S. P. DenBaars and S. Nakamura, *Appl. Phys. Lett.*, 2004, **84**, 855.
- 6 M. Ma, F. W. Mont, X. Yan, J. Cho, E. F. Schubert, G. B. Kim and C. Sone, *Opt. Express*, 2011, **19**, 1135.
- 7 S. Chhajed, W. Lee, J. Cho, E. F. Schubert and J. K. Kim, *Appl. Phys. Lett.*, 2011, **98**, 071102.
- 8 J. M. Morancho, A. Cadenato, X. Fernández-Francos, J. M. Salla and X. Ramis, *J. Therm. Anal. Calorim.*, 2008, **92**, 513.
- 9 *Essentials of Physics*, ed. J. D. Cutnell and W. J. Kenneth, Wiley, 2006.
- 10 X. F. Yang, Q. Shao, L. L. Yang, X. B. Zhu, X. L. Hua, Q. L. Zheng, G. G. Song and G. Q. Lai, *J. Appl. Polym. Sci.*, 2013, **127**, 1717.
- 11 Y. Zhang, X. Yang, X. J. Zhao and W. Huang, *Polym. Int.*, 2012, **61**, 294.
- 12 E. Vanlathem, A. W. Norris, M. Bahadur, J. DeGroot and M. Yoshitake, *Proc. SPIE*, 2006, **6192**, 619202.
- 13 K. Miyoushi, *US Pat.*, 0116640, 2004.
- 14 A. Sellinger and R. M. Laine, *Macromolecules*, 1996, **29**, 2327.
- 15 D. B. Cordes, P. D. Lickiss and F. Rataboul, *Chem. Rev.*, 2010, **110**, 2081.
- 16 K. Tanaka and Y. Chujo, *Polym. J.*, 2013, **45**, 247.
- 17 K. Tanaka, F. Ishiguro and Y. Chujo, *Polym. J.*, 2011, **43**, 708.
- 18 R. H. Baney, M. Itoh, A. Sakakibara and T. Suzuki, *Chem. Rev.*, 1995, **95**, 1409.
- 19 S. S. Choi, A. S. Lee, H. S. Lee, H. Y. Jeon, K. Y. Baek, D. H. Choi and S. S. Hwang, *J. Polym. Sci., Part A: Polym. Chem.*, 2011, **49**, 5012.
- 20 S. D. Bhagat, J. Chatterjee, B. Chen and A. E. Stiegman, *Macromolecules*, 2012, **45**, 1174.
- 21 V. S. Khire, T. Y. Lee and C. N. Bowman, *Macromolecules*, 2007, **40**, 5669.
- 22 K. M. Schreck, D. Leung and C. N. Bowman, *Macromolecules*, 2011, **44**, 7520.
- 23 A. Dondoni, *Angew. Chem., Int. Ed.*, 2008, **47**, 8995.
- 24 C. J. Kloxin, T. F. Scott, H. Y. Park and C. N. Bowman, *Adv. Mater.*, 2011, **23**, 1977.
- 25 H. Lin, X. Wan, X. S. Jiang, Q. K. Wang and J. Yin, *Adv. Funct. Mater.*, 2011, **21**, 2960.
- 26 H. Lin, X. Wan, X. S. Jiang, Q. K. Wang and J. Yin, *J. Mater. Chem.*, 2012, **22**, 2616.
- 27 W. Groh and A. Zimmermann, *Macromolecules*, 1991, **24**, 6660.
- 28 A. K. O'Brien, N. B. Cramer and C. N. Bowman, *J. Polym. Sci., Part A: Polym. Chem.*, 2006, **44**, 2007.
- 29 *Sapphire*, ed. E. R. Dobrovinskaya, L. A. Lytvynov and V. Pishchik, Springer, 2009.
- 30 J. C. Lotters, W. Olthuis, P. H. Veltink and P. Bergveld, *J. Micromech. Microeng.*, 1997, **7**, 145.
- 31 J. C. McDonald and G. M. Whitesides, *Acc. Chem. Res.*, 2002, **35**, 491.